Diamond & Related Materials 43 (2014) 66–71

Contents lists available at ScienceDirect

Diamond & Related Materials

journal homepage: www.elsevier.com/locate/diamond

Characterization and hydrogen storage in multi-walled carbon nanotubes grown by aerosol-assisted CVD method

Edgar Mosquera [a,*], Donovan E. Diaz-Droguett [b], Nicolás Carvajal [a], Martin Roble [b], Mauricio Morel [a], Rodrigo Espinoza [c]

[a] Laboratorio de Materiales a Nanoescala, Departamento de Ciencia de los Materiales, Facultad de Ciencias Físicas y Matemáticas, Universidad de Chile, Tupper Av. 2069, Santiago, Chile
[b] Instituto de Física, Pontificia Universidad Católica de Chile, Casilla 306, Santiago, Chile
[c] Laboratorio de Cerámicas Avanzadas, Departamento de Ciencia de los Materiales, Facultad de Ciencias Físicas y Matemáticas, Universidad de Chile, Tupper Av. 2069, Santiago, Chile

ARTICLE INFO

Article history:
Received 22 April 2013
Received in revised form 27 July 2013
Accepted 25 January 2014
Available online 2 February 2014

Keywords:
Camphor/alcohol
Ni/zeolite support
AACVD
Carbon nanotubes
Raman spectroscopy
Hydrogen storage capacity

ABSTRACT

The characterization and hydrogen storage capacity of multi-walled carbon nanotubes (MWCNTs) have been studied in the present work. MWCNTs with high purity and bulk yield were achieved from a mixture of camphor/alcohol on a Ni/zeolite support by aerosol-assisted chemical vapor deposition (AACVD). The morphology, surface quality and structure of MWCNTs were characterized by transmission electron microscopy (TEM). Crystallinity and defects of the MWCNTs were studied by Raman spectroscopy and thermo gravimetric analysis (TGA). Hydrogen storage properties of MWCNTs were investigated using a quartz crystal microbalance (QCM). Values between 1.2 and 2.0 wt.% of adsorbed H_2 were reached depending on the exposure pressure. The results also showed that the remaining zeolite present in the as-prepared MWCNT powder adsorbs hydrogen, allowing better adsorption performance of the CNT12 and CNT13 samples. The hydrogen adsorption behavior of CNTs is significantly affected by their structural and morphological characteristics.

1. Introduction

Carbon nanotubes (CNTs) are among the most interesting materials in current nanotechnological research, due to their low chemical activity, high aspect to ratio, high mechanical strength, and conductivity [1]. There have been extensive reports in recent years to demonstrate the growth of CNTs under different conditions [2–4]. Among CNTs synthesis methods, chemical vapor deposition (CVD) is the most suitable and economic method at low temperatures and ambient pressure when compared with laser, or arc process [5]. However, these methods are associated with a low yield and the formation of many undesired products [5]. On the other hand, aerosol assisted chemical vapor deposition (AACVD) offers more opportunities to obtain larger amounts of CNTs. Using AACVD, various inorganic porous materials were also investigated as support materials by researchers in producing single- and multi-walled CNTs [2,3]. These studies showed that the resulting structure, the morphology and applications are dependent on the experimental conditions [2,3]. The applications for CNTs have enormous potentials such as novel nanoscale electronic devices, electron field emitters, energy storage and energy conversion devices, sensors, and lithium ion batteries [4–7]. Recently, attention has focused on carbon-based materials due to the usage of CNTs as a safe hydrogen storage medium [5,8–11]. To date, many studies have revealed that hydrogen storage capacity is enhanced by added metals to carbon structures, such as Fe, Ni, Co, Cu, Au, Ag, Pt, Ca, Li, K, Al and Pd [3,5,12–14] or by using CNT-based composites [15–17]; however, the properties of hydrogen storage in these materials is still being researched at a basic level. Actually, the reproducibility of the reported hydrogen storage capacity of CNTs is poor, and the mechanism of how hydrogen is stored in CNTs remains unclear [8]. Liu et al. pointed out that certain amount of hydrogen (less than 1.7 wt.% under a pressure of ~12 MPa and at room temperature) can be stored in CNTs [8], which indicate that CNTs cannot fulfill the benchmark of 6.5 wt.% set by the U.S. Department of Energy (DOE) for hydrogen storage systems [8,13,18]. Recently, very low values of hydrogen storage capacity of CNTs started to emerge, in particular, those experimentally obtained at room temperature. The reproducibility of the reported high hydrogen capacity of CNTs is poor, and the mechanism of how the hydrogen is stored in CNTs remains unclear [8]. However, experimental studies on hydrogen storage of CNTs and CNT-based hybrid structures, as well as, the hydrogen adsorption mechanism and hydrogen adsorption sites are studied [5,13].

In the present work, synthesis of MWCNTs has been obtained in an AACVD process under nitrogen and argon flow, and their hydrogen adsorption capacity at room temperature under different loading pressures were studied. Zeolite is investigated as a suitable support for

* Corresponding author. Tel.: +56 2 978 4795; fax: +56 2 699 4119.
E-mail address: edemova@ing.uchile.cl (E. Mosquera).

http://dx.doi.org/10.1016/j.diamond.2014.01.016
0925-9635/

growing CNTs and storing hydrogen, allowing better adsorption performance in between carbon nanotubes. Transmission electron microscopy (TEM), thermal gravimetric analysis (TGA) and Raman spectroscopy were used to evaluate the structure, grade of graphitization and quality characteristics of MWCNTs.

2. Experimental details

2.1. Preparation of MWCNT

MWCNTs were synthesized using an aerosol-assisted CVD method. Approximately 2.0 g of camphor, mixed with 10 mL of isopropyl alcohol were placed in an ultrasonic nebulizer. Pure nitrogen (N_2) and argon (Ar) gas were used to transport the precursor mist generated in the atomization chamber to a horizontal quartz tube (length: 50 cm, diameter: 3.0 cm) inserted in a furnace. For CNT12 and CNT13 samples, nickel particles were used as catalyst impregnated in zeolite (molecular sieve: alkalimetal aluminum silicate/calcium, Chromatograph grade, linde/Coast engineering laboratory/Redondo Beach CA-USA). While for CNT11, only nickel particles were employed, as shown in Table 1. The mist (camphor mixed with alcohol) was pyrolyzed over catalyst-pregnated zeolite at 800 °C under a flow of 1 L/min for 20 min. When the system was cooled naturally to room temperature (RT), the blackened zeolite was collected for characterization.

2.2. Sample characterization

Structural characterization was done with a high-resolution transmission electron microscope (HRTEM, Tecnai F20 FEG-S/TEM) operated at 200 kV. TEM samples were ultrasonically dispersed in isopropyl alcohol and then collected in an ultrathin holey carbon-coated Cu grid. Thermogravimetric analysis (TGA) of blackened zeolite was performed with a TA Instruments, TGA Q50, under nitrogen gas and heated from room temperature (RT) to 800 °C with the heating rate of 10 °C/min. Micro-Raman spectra were recorded at RT on a LabRam 010 from ISA using a He–Ne laser with wavelength of 632.8 nm at 5.5 mW. The Raman system uses a backscattering geometry, where the incident beam is linearly polarized and the spectral detection unpolarized. The objective lens of the microscope was an Olympus Mplan10× (numerical aperture 0.9).

As-prepared MWCNT powders grown by aerosol-assisted CVD were deposited at RT on top-face of a microbalance quartz crystal (QC) used as support-substrate. The powder was dispersed in isopropyl alcohol using an ultrasonic bath for 7 min. The suspension formed was deposited using a dropper onto the QC and then dried to room air at RT. Then, the QC was located in the head of a quartz crystal microbalance system (from MDC model SQM-310) placed inside a vacuum chamber. The chamber was pumped down to 7×10^{-6} Torr using turbo and rotatory pumps. A gate valve placed between the chamber and the turbo pump to isolate the chamber from the vacuum, allowed pressurizing with hydrogen gas injecting it through a needle valve. The mass changes upon hydrogen adsorption were determined by in-situ monitoring of the changes in the resonance frequency of the QC as function of time while the sample was exposed to hydrogen for 8 min. After H_2 exposure, the chamber was again pumped down to 7×10^{-6} Torr, the process was repeated by injecting hydrogen until reaching a higher pressure. Increasing pressures between 3 and 45 Torr (measured with a capacitive gauge, Baratron from MKS instruments) were used in the different hydrogenation cycles for studying the pressure effect on the hydrogen storage behavior at RT of the MWCNTs.

The relationship between the mass added to the QC due to the H_2 adsorption by the CNTs and the shift in its resonance frequency, Δf, is represented by the Sauerbrey's equation [19–21]:

$$\Delta f = -\frac{2f^2}{A\sqrt{\rho \times \mu}}\Delta m$$

where f is the QC resonant frequency, ρ is the density, μ is the shear modulus of the QC and A is the area covered by the mass. This equation indicates that a negative variation of the resonance frequency is due to a mass gain. Details about the use of this equation and method for the determination of mass gained by a QC can be found in [22] where a study of hydrogen absorption in films and Pd clusters using a microbalance quartz crystal system was reported.

3. Results and discussion

Apart from the first studies on the synthesis of CNTs, there are plenty of reports using thermal decomposition of many hydrocarbons on zeolites (such as Y-type high-silica zeolite (HSZ-390HUA), or aluminophosphate crystals (AFI))) as mesoporous substrates or support [2]. However, it is difficult to compare the present results with those reported, because the CVD method presents more sensitive parameters and conditions (temperature, flow, gas carrier) on CNTs production. However, from the viewpoint of the present research, the results obtained using camphor/alcohol as precursor material, are comparable with other results in the production of CNTs on a large scale. Most precursors used for the synthesis of CNTs are derived from hydrocarbons such as methane, ethane, acetylene, benzene, ethanol, as well as some alkyl chains (C_{12} and C_{16} alkanes) [23] which have been used as carbon sources of CNT synthesis. However, these precursors do not exhibit a high performance in the synthesis of CNTs.

Comparing camphor ($C_6H_{16}O$) with the most commonly used CNT precursors, Kumar et al. [2,3] reported mass production of CNTs from camphor using CVD, and established the growth condition of MWCNTs and SWCNTs using Fe–Co catalyst impregnated in zeolite support. MWCNTs were grown at a temperatures as low 550 °C, whereas SWCNTs were grown at 900 °C. These studies confirm that SWCNTs or MWCNTs can be selectively grown by proper selection of catalyst materials and their concentration [3].

Based on the above, it was found that for the synthesis of CNTs using a mixture of camphor/alcohol, the performance is dependent on the catalyst materials, gas carrier, and support used. TEM micrographs of the MWCNTs are shown in Figs. 1 and 2. Fully growth of MWCNTs was obtained when N_2 was used as gas carrier (Fig. 1). Fig. 2 shows TEM images of MWCNTs made by AACVD using argon as gas carrier. These images clearly reveal that the formed products are nanotubes with average diameters of 20 nm and 200 nm for CNT12 and CNT13, respectively. As shown in Fig. 1(a–d), Ni particles were attached on the tips of the CNTs, indicating the formation of graphene shells around the Ni particles and the continuous movements of the Ni particles produced the CNTs. While in Fig. 2(a–d), the CNTs presented chain structures when they were synthesized with argon. Ni-filled CNTs and their chain structures were formed, as shown in Fig. 2(a). Some defects are observed on the graphitic layers. Furthermore, most of the outer surface of the tube

Table 1
Experimental condition, intensity ratio of Raman spectra and hydrogen storage capacity of MWCNTs.

Sample	Catalyst	Support	Carrier gas	Intensity ratio (I_D/I_G)	Intensity ratio ($I_{G'}/I_G$)	H_2 storage capacity (wt.%)
CNT11	Ni	–	N_2	1.02	0.50	1.5
CNT12	Ni	Zeolite	N_2	0.77	0.82	1.7
CNT13	Ni	Zeolite	Ar	0.63	0.84	2.1

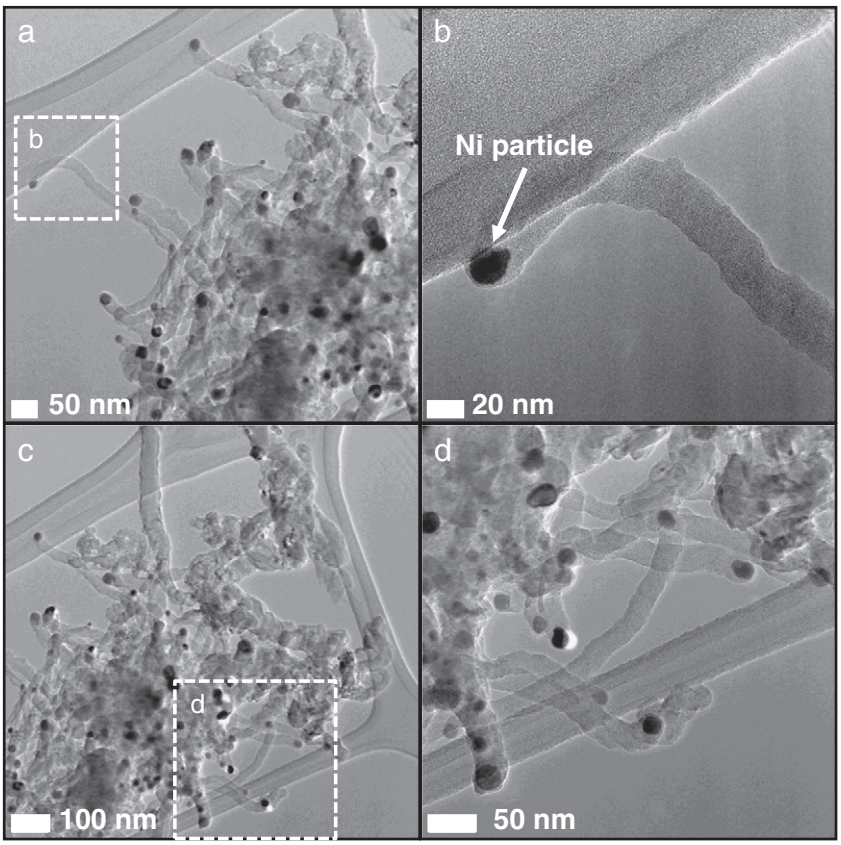

Fig. 1. TEM images of the MWCNTs produced by AACVD of a mixture camphor/alcohol. (a, c) Low magnification TEM images of the CNT12. (b, d) Zoom of the dotted frame in (a) and (b), showing nickel particle on the tips of the CNTs.

wall is free of amorphous carbon layer (Fig. 2(e,f)). When argon is used, the ordered structures are destroyed and large numbers of defects are presented in the graphitic layers. Thus, there is a lower crystallinity. The high-magnification TEM image shows that many small defects are observed on the surface of CNTs, and the degree of crystallinity decreases.

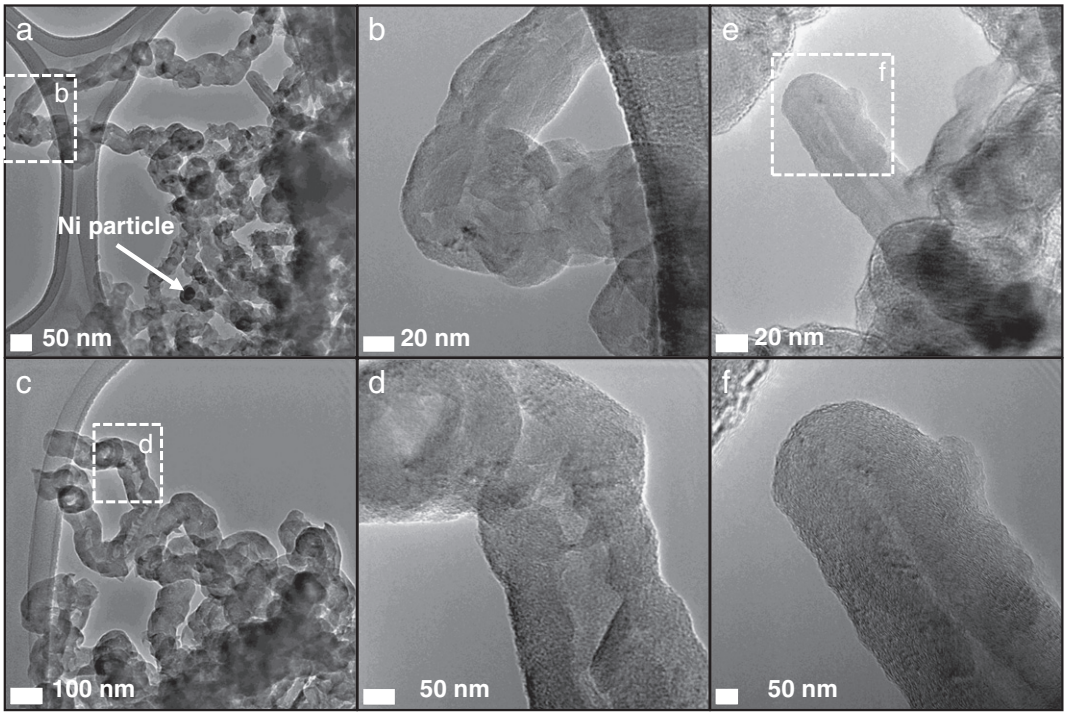

Fig. 2. (a–f) TEM images of CNT13 produced by AACVD. (b) The dotted frame in (a) with increased magnification. Panels (d) and (f) zoom from the dotted frames in (c) and (e) shown two as-grown CNTs.

The CNT purity was determined based on thermogravimetric analysis (TGA) of an as-grown sample from room temperature to 800 °C at 10 °C/min. Fig. 3 shown that an initial weight loss of around 0.20–0.25% within the 60–100 °C temperature range, which may be due to the removal of volatile organic impurities inherited with the base support material. On the other hand, Fig. 3 showed that thermal degradation started at 613 °C (CNT11), 567 °C (CNT12), and 689 °C (CNT13), and was completely decomposed around 800 °C. The TGA weight loss suggests that the purity of CNTs is >96%. Nevertheless, the TGA data shown as well that the CNTs grown over zeolite and nickel (CNT12 and CNT13) support had a higher percentage of residual metal. The amount of metal catalyst in the sample of nanotubes has been shown to affect the combustion rate and the onset of oxidation temperature [24]. The higher oxidation onset temperature for the CNTs grown indicates a low graphitization degree and presence of a many defects and disorder.

Raman scattering has been performed to confirm the degree of crystallinity of the nanotubes. Fig. 4 shows the Raman spectra of the MWCNTs. As shown in Fig. 4, two distinct peaks were observed at about 1325 and 1579 cm^{-1} corresponding respectively to the disorder of the graphite structure (D-band (I_D)) and to the high-frequency E_{2g} firs-order mode of graphite structure (G-band (I_G)). The intensity ratio (I_D/I_G) is indicative of the crystallinity of the nanotubes [1,4]. From the Raman spectra in Fig. 4 and Table 1, a lower intensity ratio I_D/I_G of 1.02 (CNT11), 0.77 (CNT12), and 0.63 (CNT13) have been established, lower than the ratios reported by Bao et al. [1], respectively; this is a signature of the defects contained in graphene walls and a low degree of crystallinity. In addition, there is a weak G' band at 2660 cm^{-1}, indicating a very poor order for the CNTs. The ratio of G' band to G band ($I_{G'}/I_G$) is also calculated to estimate the quality of the CNTs (Table 1). These results of Raman spectroscopy are in good agreement with our TEM and TGA observation. Many researchers reported that defect sites in CNTs could adsorb hydrogen molecules in comparison to ideal hexagonal structures of CNTs [13].

We examined the hydrogen storage properties of the as-prepared CNTs. Fig. 5 shows the weight percentage of H_2 adsorbed at RT by the

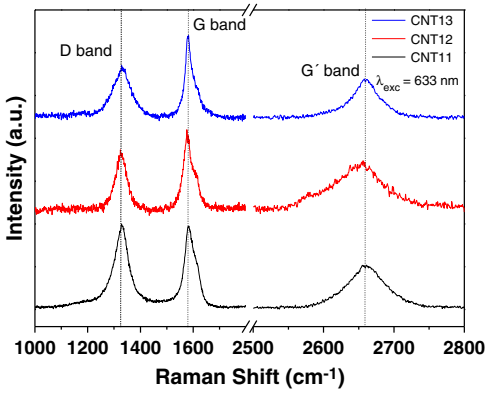

Fig. 4. Raman spectra of MWCNTs grown by AACVD.

MWCNTs when exposed to successive cycles of H_2 increasing pressures ranging between 3 and 45 Torr. A sample composed only of zeolite powder was used for studying the effect of the presence of this microporous aluminosilicate used as support during the growth of some samples on the H_2 storage capacity. The simple hydrogen injection process into the vacuum chamber induces a shift of the QC resonance frequency not associated to mass gain by hydrogen adsorption of the samples. To rule out this effect and a possible error in the determination of the amount of hydrogen adsorbed shown in Fig. 5, a bare microbalance quartz crystal was exposed to the same cycles of loading and hydrogen unloading performed on the CNTs samples. We found that the QC resonance frequency was shifted about 3.3 Hz when the chamber was filled with hydrogen. Therefore, this frequency shift was subtracted from the values determined using the CNT samples.

Fig. 5 shows that the three samples of MWCNTs exhibit different adsorption behaviors upon H_2 exposure. The sample CNT11 reached 1.4 wt.% during the first exposure using just 3 Torr of H_2, value that did not vary significantly with increased H_2 pressure, where percentages between 1.2 and 1.5 were obtained. On the contrary, the samples

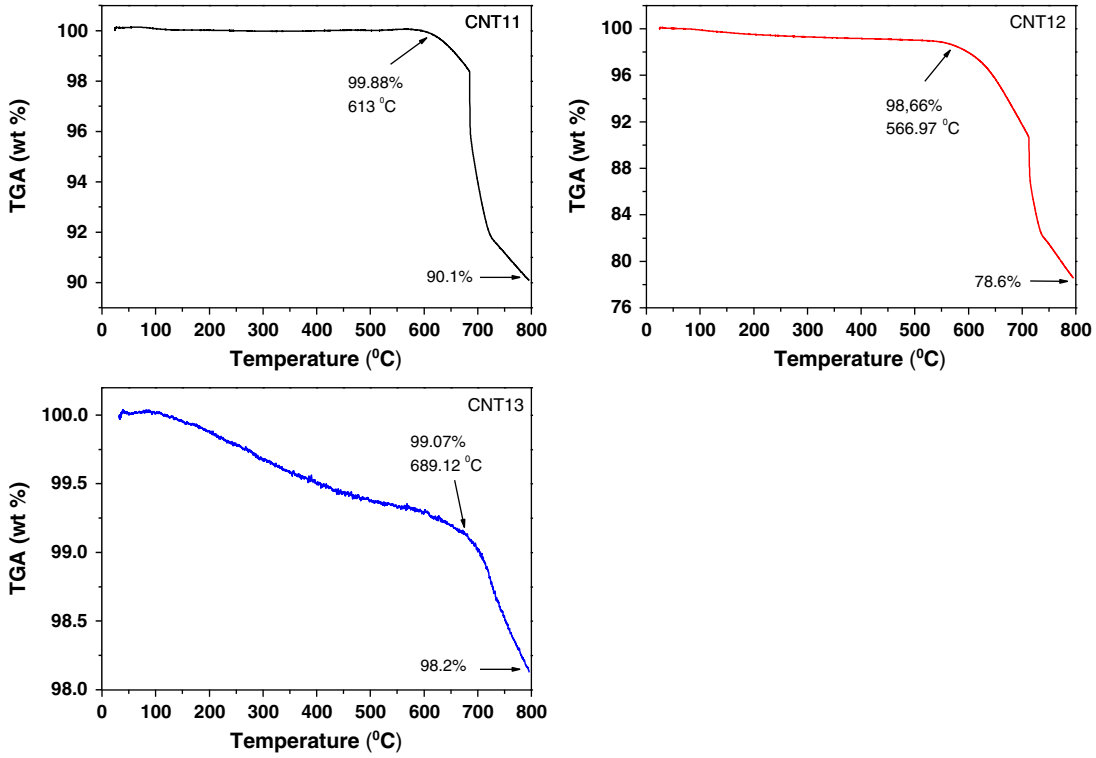

Fig. 3. Thermogravimetric analysis of the MWCNTs grown at 800 °C on nickel impregnated in zeolite.

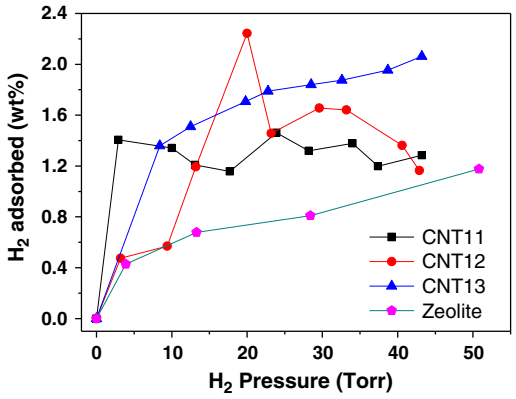

Fig. 5. Hydrogen storage capacity at RT from the MWCNTs exposed to various H_2 pressures. A sample composed only of zeolite was used as comparison.

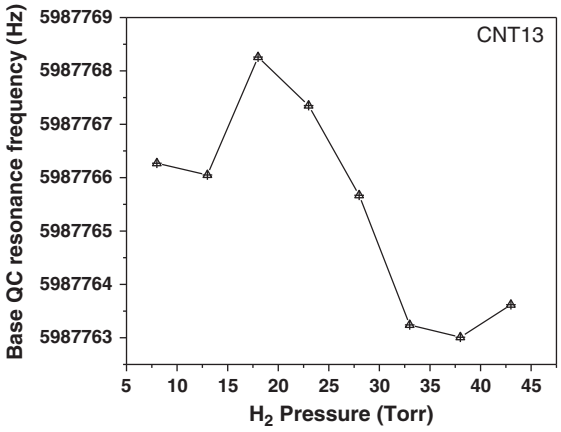

Fig. 6. Values of base resonance frequency of quartz crystal for the sample CNT13 recorded during different hydrogen exposure cycles.

CNT12 and CNT13 showed dependence regarding the H_2 pressure. The weight percentage values of the sample CNT12 increased significantly between 3 and 20 Torr reaching a maximum of about 2.3 at 20 Torr, as depicted in Fig. 5. Then, the adsorbed H_2 dropped at higher pressures down to 1.2 at 43 Torr. The peak at 20 Torr is attributed to a sudden filling of the MWCNTs and voids generated among the agglomerated carbon nanotubes as well as to a stress effect of the first monolayer of adsorbed H_2 leading to a higher value in the QC resonance frequency and, therefore, of mass gained [25]. The sample CNT13 showed a gradual increase of the H_2 amount adsorbed as pressure increased reaching a maximum value of about 2.1 at the highest exposure pressure of 43 Torr. These weight percentages are comparable or higher than other reported values of H_2 storage capacities at RT by non-pretreated/doped carbon nanotubes [8,12,18,26–30]. Finally, the last curve corresponding to a sample made of zeolite indicates that the microporous aluminosilicate particles adsorb hydrogen, which increased as pressure increased. The porous character of the zeolite with pore diameter as small as 2 nm increases the specific surface area of whole sample and the pore-channels formed help to provide more adsorption sites for the hydrogen molecule. This would help to understand the better H_2 adsorption capacity of the samples CNT12 and CNT13, which contain zeolite particles, mixed with carbon nanotubes. On the other hand, these results of hydrogen adsorption performance from the samples are correlated with their structural and morphological characteristics. The samples CNT12 and CNT13 with lower crystallinity degree and higher presence of defects exhibit a better H_2 storage capacity, in fact, the sample CNT13 with larger average diameter of the carbon tubes and minor walls graphitization revealed the best behavior upon H_2 exposure. This would corroborate the thesis that defect sites, tube width and low crystallinity would promote an enhancement in the H_2 storage properties of the MWCNTs.

The reversible character of the hydrogen adsorption–desorption process at RT in these CNT samples when the vacuum chamber is loaded and gas unloaded was also evaluated. The study was made monitoring for each sample the value changes of the QC resonance frequency "in vacuum" (base resonance frequency) after each loading/gas unloading cycle. The results showed that maximum differences of the base frequency between successive cycles were less than 9×10^{-5}% (~7 Hz) revealing that the CNTs practically released all the hydrogen adsorbed when the chamber is unloaded by pumping down. The changes of the base resonance frequency between successive cycles of loading and hydrogen unloading were mainly detected in the samples CNT12 and CNT13. In these cases the value decreased slightly after each cycle due mainly to the zeolite effect whose nanopores kept some hydrogen molecules occluded thus avoiding a complete desorption when a pumping down of the chamber is performed. This hydrogen partial retention led to an increase in the sample mass and, therefore, a decrease of the base QC resonance frequency (see Sauerbrey's equation). Fig. 6 shows precisely the values of the base QC resonance frequency of the sample CNT13 during the cycles performed at various hydrogen pressures.

The values of hydrogen adsorption of CNT samples (Fig. 5) are reproducible to the extent that the absorption study of a certain sample is carried out under the same experimental conditions. Same conditions mean: i) that the sample is exposed to the same process of loading and hydrogen unloading (cycles number and exposure pressures), ii) to reach the same vacuum conditions in the chamber, and iii) that the temperature of the microbalance quartz crystal is kept constant during the H_2 adsoption experiments. The latter, is very important, because the QC resonance frequency changes with the temperature variation. For this reason, special care is focused on the cooling system of the microbalance where the temperature of water used as coolant is kept constant at 19 °C.

4. Conclusion

In this study, MWCNTs were produced by AACVD using a camphor/alcohol mixture and Ni catalyst and zeolite as precursors. The identified characteristics of as-synthesized MWCNTs as well as hydrogen storage capacity were studied. TEM micrographs revealed that the formed MWCNTs have an average diameter in between 20 nm and 50 nm. Also, some defects and a low degree of crystallinity are observed on the graphitic layers. From Raman spectroscopy we conclude that the results are in good agreement with our TEM and TGA observation. The H_2 storage results showed that the samples grown using zeolite in the support together with a lower crystallinity of their carbonaceous structure exhibit higher values of adsorbed H_2 (weight percentages), as well as a behavior dependent on the hydrogen pressure.

Primary novelty statement

Hydrogen adsorption capacities of multi-wall carbon nanotubes (MWCNTs) at room temperature under loading pressures were studied. Defects and a low degree of crystallinity are observed on the graphitic layers by TEM, TGA and RS. The defects sites, the tube width and the low crystallinity would promote an enhancement in the H2 storage properties of the MWCNTs.

Acknowledgments

This work was partially supported by the Chilean Government Research Agencies FONDECYT (Grant no. 11110001) and CONICYT (Grant no. ACT1117). The authors thank Professor Alejandro Cabrera from Physics Department of the Pontifícia Universidad Católica de Chile for the provision of laboratory equipments for this research.

References

[1] J. Bao, N. Kishi, I. Khatri, T. Soga, T. Jimbo, Catalyst-free synthesis of carbon nanofibers by ultrasonic spray pyrolysis of ethanol, Mater. Lett. 68 (2012) 240–242.
[2] M. Kumar, Y. Ando, Controlling the diameter distribution of carbon nanotubes grown from camphor on a zeolite support, Carbon 43 (2005) 533–540.
[3] M. Kumar, Y. Ando, Chemical vapor deposition of carbon nanotubes: a review on growth mechanism and mass production, J. Nanosci. Nanotechnol. 10 (2010) 3739–3758.
[4] F.-W. Wang, T.-C. Lin, S.-D. Tzeng, C.-T. Chou, Field emission properties of carbon nanotube cathodes produced using composite plating, Appl. Surf. Sci. 256 (2010) 7600–7605.
[5] K.-S. Lin, Y.-J. Mai, S.-R. Li, C.-W. Shu, C.-H. Wang, J. Nanomater. (2012) 1 (2012 Article ID 939683).
[6] S.L. Katar, A. Biaggi-Labiosa, A.E. Plaud, E. Mosquera-Vargas, L. Fonseca, B.R. Weiner, G. Morell, Silicon encapsulated carbon nanotubes, Nanoscale Res. Lett. 5 (2010) 74–80.
[7] S.L. Katar, D. Hernandez, A. Biaggi-Labiosa, E. Mosquera-Vargas, L. Fonseca, B.R. Weiner, G. Morell, SiN/bamboo like carbon nanotube composite electrodes for lithium ion rechargeable batteries, Acta 55 (2010) 2269–2274.
[8] C. Liu, Y. Chen, C.-Z. Wu, S.-T. Xu, H.-M. Cheng, Hydrogen storage in carbon revisited, Carbon 48 (2010) 452–455.
[9] Z. Liu, Q. Xue, C. Ling, Z. Yan, J. Zheng, Hydrogen storage and release by bending carbon nanotubes, Comput. Mater. Sci. 68 (2013) 121–126.
[10] M.A. Rafiee, The Study of hydrogen storage in carbon nanotubes using calculated nuclear quadrupole coupling constant (NQCC) parameters (a theoretical ab initio study), J. Comput. Theor. Nanosci. 9 (2012) 2021–2026.
[11] X.-L. Sheng, H.-J. Cui, F. Ye, Q.-B. Yan, Q.-R. Zheng, G. Su, Octagraphene as a versatile carbon atomic sheet for novel nanotubes,unconventional fullerenes, and hydrogen storage, J. Appl. Phys. 112 (2012) (074315-074315-7).
[12] H.-M. Cheng, Q.-H. Yang, C. Liu, Hydrogen storage in carbon nanotubes, Carbon 39 (2001) 1447–1454.
[13] A. Reyhani, S.Z. Mortazavi, S. Mirershadi, A.Z. Moshfegh, P. Parvin, A. NozadGolikand, Hydrogen storage in decorated multiwalled carbon nanotubes by Ca, Co, Fe, Ni, and Pd nanoparticles under ambient conditions, J. Phys. Chem. C 115 (2011) 6994–7001.
[14] H.L. Wang, X.L. Cheng, H. Zhang, Y.J. Tang, Very high hydrogen storage capacity of Al-adsorbed single walled carbon nanotube (SWCNT): multi-layer structure of hydrogen molecules, Int. J. Mod. Phys. B 27 (2013) 1350061–1350072.
[15] D. Silambarasan, V.J. Surya, V. Vasu, K. Iyakutti, One-step process of hydrogen storage in single walled carbon nanotubes-tin oxide nano composite, Int. J. Hydrogen Energy 38 (2013) 4011–4016.
[16] N. Rahimi, M.M. Doroodmand, S. Sabbaghi, M.H. Sheikhi, Electrochemical hydrogen storage of Pt and Ni nanoparticles-electrodeposited multi-walled carbon nanotube/micro-hybrid composite, J. Electroanal. Chem. 689 (2013) 297–302.
[17] A.H. Noroozi, S. Safa, R. Azimirad, H.R. Shirzadi, N.G. Yazdi, Microstructure and Hydrogen storage properties of lani$_5$-multi wall carbon nanotubes (MWCNTs) composite, Arab. J. Sci. Eng. 38 (2013) 187–194.
[18] S. Banerjee, S. Murad, I.K. Puri, Hydrogen storage in carbon nanostructures: possibilities and challenges for fundamental molecular simulations, Proc. IEEE 94 (2006) 1806.
[19] T.G. Sauerbrey, Verwendug von Schwingquarzen zur Wägung dünner Schichten und zur Microwägung, Z. Phys. 155 (1959) 206–222.
[20] V.M. Mecea, From quartz crystal microbalance to fundamental principles of mass measurements, Anal. Lett. 38 (2005) 753–767.
[21] R. Lucklum, P. Hauptmann, The quartz microbalance: mass sensitivity, viscoelasticity and acoustic amplification, Sensors Actuators B 70 (2000) 30–36.
[22] R. El Far, D.E. Diaz-Droguett, S. Rojas, J.I. Avila, C.P. Romero, P. Lievens, A.L. Cabrera, Quantitative determination of hydrogen absorption by Pd cluster-assembled films using a quartz cristalmicrobalance, Thin Solid Films 52 (2012) 199–203.
[23] C. Zhuo, B. Hall, H. Richter, Y. Levendis, Synthesis of carbón nanotubes by sequential pyrolysis and combustion of polyethylene, Carbon 48 (2010) 4024–4034.
[24] D. Bom, R. Andrew, D. Jacques, J. Antony, B. Chen, M.S. Meier, J.P. Selegue, Thermogravimetric analysis of the oxidation of multiwalled carbon nanotubes: evidence for the role of defect sites in carbon nanotube chemistry, Nano Lett. 2 (2002) 615–619.
[25] C.L. Wang, J. Krim, M.F. Toney, Roughness and porosity characterization of carbon and magnetic films through adsorption isotherm measurements, J. Vac. Sci. Technol. A 7 (1989) 2481–2485.
[26] S.C. Lim, K.K. Kim, S.H. Jeong, K.H. An, S.-B. Lee, Y.H. Lee, Dual quartz crystal microbalance for hydrogen storage in carbon nanotubes, Int. J. Hydrogen Energy 32 (2007) 3442–3447.
[27] P.-X. Hou, S.-T. Xu, Z. Ying, Q.-H. Yang, C. Liu, H.-M. Cheng, Hydrogen adsorption/desorption behavior of multiwalled carbon nanotubes with different diameters, Carbon 41 (2003) 2471–2476.
[28] H. Zhu, A. Cao, X. Li, C. Xu, Z. Mao, D. Ruan, J. Liang, D. Wu, Hydrogen adsorption in bundles of well-aligned carbon nanotubes at room temperature, Appl. Surf. Sci. 178 (2001) 50–55.
[29] W.Z. Huang, X.B. Zhang, J.P. Tu, F.Z. Kong, J.X. Ma, F. Liu, H.M. Lu, C.P. Chen, The effect of pretreatments on hydrogen adsorption of multiwalled carbon nanotubes, Mater. Chem. Phys. 78 (2002) 144–148.
[30] K. Shen, H. Xu, Y. Jiang, T. Pietraß, The role of carbon nanotube structure in purification and hydrogen adsorption, Carbon 42 (2004) 2315–2322.